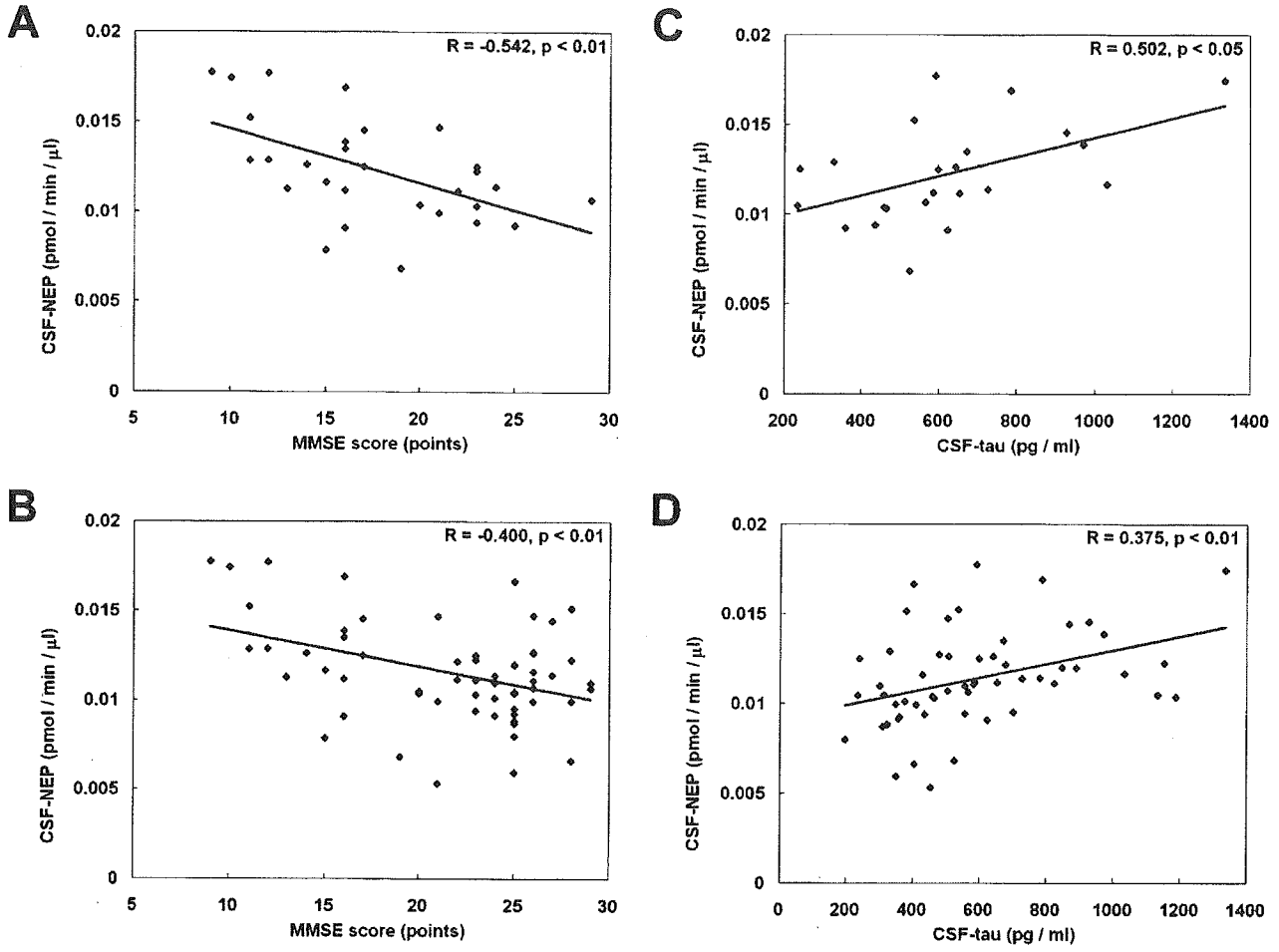

Fig 2. Association of cerebrospinal fluid neprilysin activity (CSF-NEP) (CSF-NEP) with disease severity assessed by Mini-Mental State Examination (MMSE) score and CSF-tau level in patients with progressive mild cognitive impairment (pMCI) and Alzheimer's disease (AD). (A) CSF-NEP was increased with disease progression in AD patients and was significantly correlated with MMSE score. (B) A significant correlation between CSF-NEP and MMSE score was also observed when patients with pMCI were added to the study group. (C) CSF-NEP showed a significant and positive correlation with CSF-tau in AD patients. (D) Correlation between CSF-NEP and CSF-tau levels remained significant when patients with pMCI were also included in the analysis. Solid lines *represent the linear regression of the data.*

cantly decreased in pMCI patients (0.0108 ± 0.0004pmol/min/µl; mean ± SE) compared with subjects in the control group (0.0146 ± 0.0008pmol/min/µl). There also was a significant decrease of CSF-NEP in AD patients (0.0121 ± 0.0005pmol/min/µl) compared with the control group. When the AD patients were subdivided into mild (MMSE scores, >17 points) and moderate AD groups (MMSE scores, 9–17 points), patients with mild AD showed a significant reduction of CSF-NEP (0.0107 ± 0.0006pmol/min/µl) relative to the control subjects (see Fig 1E). By contrast, CSF-NEP in patients with moderate AD (0.0132 ± 0.0007pmol/min/µl) was similar to the control level (see Fig 1E). Alteration of CSF-NEP during progression of AD was more intensively analyzed by plotting CSF-NEP data in AD patients against their MMSE scores. Notably, levels of CSF-NEP in AD patients showed a significant inverse correlation with MMSE scores (Fig 2A). The correlation remained significant after data from pMCI patients were added to the plot (see Fig 2B). Thus, it is conceivable that occurrence of a prominent CSF-NEP reduction is confined to early stages of AD pathogenesis, and thereafter CSF-NEP is likely to be reversed to greater levels with advance of the disease.

AD patients with high levels of CSF-NEP showed higher levels of CSF-tau, thus the correlation between the two variables was significant (see Fig 2C). There also was a significant correlation between CSF-NEP and CSF-tau when patients with pMCI were combined with AD patients for analysis (see Fig 2D). Because CSF-tau is supposed to increase as a function of cytoskeletal disruption and abnormal tau accumulation in neurons, these findings support an increased diffusion of neuronal

neprilysin to the extracellular matrix and CSF as a consequence of injuries of neuronal membranes.

CSF-NEP was unrelated to CSF-Aβ42 in AD patients ($R = -0.112$, $p > 0.05$; data not shown), whereas correlation between these two variables became significant when patients with AD and pMCI were included for analysis ($R = -0.262$, $p < 0.05$; data not shown).

CSF-NEP was not correlated with age and sex in any of the studied groups. In addition to the aforementioned simple correlation analyses, multiple regression with stepwise selection option was used as an exploratory tool for identification of primary factors that determine levels of CSF-NEP in patients with pMCI and AD. As listed in Table 2, MMSE score and CSF-tau were selected as independent variables. CSF-tau showed the greatest partial correlation to CSF-NEP, and MMSE score also had a tendency to be correlated to CSF-NEP. Other variables, including age, sex, and CSF-Aβ42 were eliminated by the stepwise selection; thus, it is likely that the marked influence of the disease severity on both CSF-NEP and CSF-Aβ42 produced an apparent correlation between these two CSF measures in the simple correlation analysis.

CSF-NEP in sMCI subjects (0.0147 ± 0.001pmol/min/μl) was similar to that in control subjects ($p > 0.05$) and was significantly greater than that in pMCI subjects ($p < 0.05$), implying applicability of CSF-NEP measurement to differentiation between pMCI and sMCI at baseline examination.

Neprilysin in CSF was further characterized by immunoblotting (Fig 3). Deglycosylated neprilysin in the brain and CSF showed the same molecular mass, which was larger than the apparent molecular weight of extracellular domain of neprilysin and corresponded to the predicted size of the full-length form. Therefore, secretion of neprilysin from neurons to the extracellular matrix likely occurs without shedding of the full-length enzyme.

Plasma-NEP did not differ among the control (1.669 ± 0.306pmol/min/μl), pMCI (1.777 ± 0.429pmol/min/μl), and AD (1.944 ± 0.395pmol/min/μl) groups. Patients with mild (2.036 ± 0.725pmol/min/μl) and moderate AD (1.816 ± 0.494pmol/min/μl) exhibited similar levels of plasma-NEP. Moreover, there was no significant correlation between levels of CSF-NEP and plasma-NEP in any of the examined groups ($R = 0.103$, $p > 0.05$; data not shown). Hence, the CSF-NEP changes in patients with pMCI and early AD observed in this study were unrelated to the status of plasma neprilysin, but they conceivably reflected an altered transfer of neprilysin from the brain to CSF in these patients. This notion was further tested by the following experiments using rAAV-treated, neprilysin-deficient mice and KA-treated rats.

Table 2. Multiple Regression Analysis for Patients with pMCI and AD

Independent Variable	Partial Correlation Coefficient	p
MMSE	−0.237	0.096
CSF-tau	0.292	0.042

$R^2 = 0.152$, F = 3.93, $p = 0.027$.
Age, sex, and CSF-Aβ42 were eliminated from independent variables by the stepwise selection.
pMCI = progressive mild cognitive impairment; AD = Alzheimer's disease; MMSE = Mini-Mental State Examination; CSF = cerebrospinal fluid.

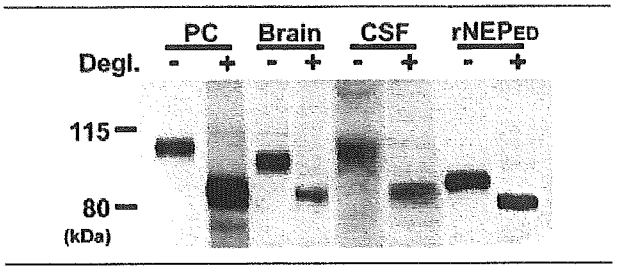

Fig 3. Biochemical characteristics of neprilysin in the brain and cerebrospinal fluid (CSF) from the human subjects. Non-deglycosylated neprilysin in the CSF sample from an AD patient migrated at approximately 95kDa, which was nearly the same as the apparent molecular mass of the human neprilysin from primary culture (PC) of cortical neurons, whereas neprilysin in the membrane-associated fraction extracted from the brain migrated slightly faster than the CSF neprilysin. After deglycosylation, the apparent molecular weight of neprilysin in the PC, brain, and CSF became approximately 85kDa, which corresponds to the predicted size of full-length, unmodified neprilysin. The recombinant extracellular domain of human neprilysin ($rNEP_{ED}$) exhibited smaller apparent molecular mass than other samples.

Physiological Transfer of Neprilysin from the Brain to Cerebrospinal Fluid Demonstrated in Mice

Neprilysin activity was assayed in the hippocampus, CSF, and plasma of neprilysin-deficient mice injected with rAAV-NEP, as well as untreated wild-type and neprilysin-deficient mice. Hippocampal neprilysin activity was nearly undetectable in the untreated neprilysin-deficient mice, whereas it prominently increased at 10 weeks after injection with rAAV-NEP (Fig 4A). There remained unnegligible signals in CSF-NEP assay for untreated neprilysin-deficient mice, which may be produced by degradation of the substrate by thiorphan semisensitive endopeptidases (see Fig 4B). In rAAV-NEP–treated, neprilysin-deficient mice, CSF-NEP showed a significant increase to approximately 70% of CSF-NEP in wild-type mice (see Fig 4B). By contrast, plasma-NEP in neprilysin-deficient mice treated with rAAV-NEP stayed at an undetectable level, similar to

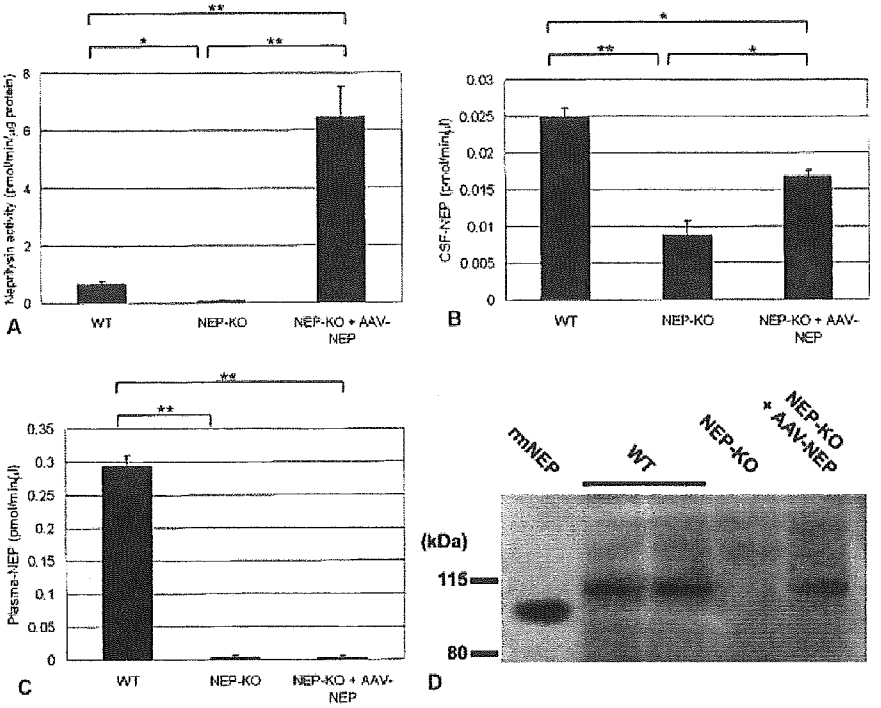

Fig 4. Physiological transfer of neprilysin from the brain into CSF demonstrated by neprilysin-deficient mice injected with recombinant adeno-associated viral vector expressing human neprilysin (rAAV-NEP). (A) Hippocampal neprilysin activity was nearly undetectable in untreated neprilysin-deficient mice (NEP-KO). By contrast, NEP-KO mice at 10 weeks after intrahippocampal rAAV-NEP injection (NEP-KO + AAV-NEP) showed a pronouncedly high level of CSF-NEP, which was approximately 10-fold greater than the endogenous neprilysin activity in wild-type (WT) mice. (B) CSF samples of NEP-KO mice did not produce overt signals compared with those of WT mice. After administration of rAAV-NEP, CSF-NEP in NEP-KO mice was increased to 70% of the endogenous level in WT mice. (C) Unlike CSF-NEP, plasma-NEP did not display an apparent increase after treatment with rAAV-NEP. (D) Immunoblotting of neprilysin in mouse CSF showed consistency with CSF-NEP assay. Each lane was loaded with either CSF sample pooled from three mice or recombinant murine neprilysin (rmNEP). Bars *represent standard error.* $^{*}p < 0.05$; $^{**}p < 0.01$.

untreated neprilysin-deficient mice (see Fig 4C). The transfer of neprilysin from the brains of rAAV-NEP–injected, neprilysin-deficient mice into CSF was also clearly demonstrated by immunoblotting of neprilysin in CSF samples (see Fig 4D). The predominance of the association between neprilysin activities in the brain and CSF over the plasma-CSF correlation suggests strong impacts of brain neprilysin activity on CSF-NEP through transfer of neuronal neprilysin into CSF in physiological conditions.

Pathological Transfer of Neprilysin from the Brain to Cerebrospinal Fluid in Kainic Acid–Treated Rats

In rats injected with KA, there was a KA-induced increase of CSF-NEP in a dose-dependent fashion; low-dose, KA-treated rats showed a slight and insignificant increase of CSF-NEP, and a pronounced increase in CSF-NEP (68-fold greater than the control level) was observed in rats treated with high-dose KA (Fig 5A). Unlike CSF-NEP, plasma-NEP did not significantly differ among the three groups (see Fig 5B). Immunoblotting of neprilysin also indicated a remarkable increase of neprilysin in CSF samples from rats treated with high-dose KA (see Figs 5C [top panel], D [left panel]). In addition to neprilysin, levels of tau in CSF were prominently increased in rats injected with high-dose KA (see Figs 5C [bottom panel], D [right panel]). These data support an aberrantly increased transfer of both neprilysin and tau from damaged brain to CSF, providing a molecular basis for the close association between CSF-NEP and CSF-tau in patients with pMCI and AD (see Figs 2C, D).

Immunoblotting of neprilysin showed that neprilysin in membrane-associated protein fraction from the hippocampi was significantly reduced in rats injected with high-dose KA (Figs 6A, B [left panel]). Neprilysin in Tris/NaCl-soluble fraction had a tendency to increase in KA-treated rats in a dose-dependent fashion, although the increase was not statistically significant (see Figs 6A, B [right panel]). Immunohistochemistry for fragmented α-spectrin indicated extensive activation of calpains in the entire hippocampus except the dentate gyrus after administration of KA at a high dose (see Figs 6C, D). A marked reduction of neprilysin immu-

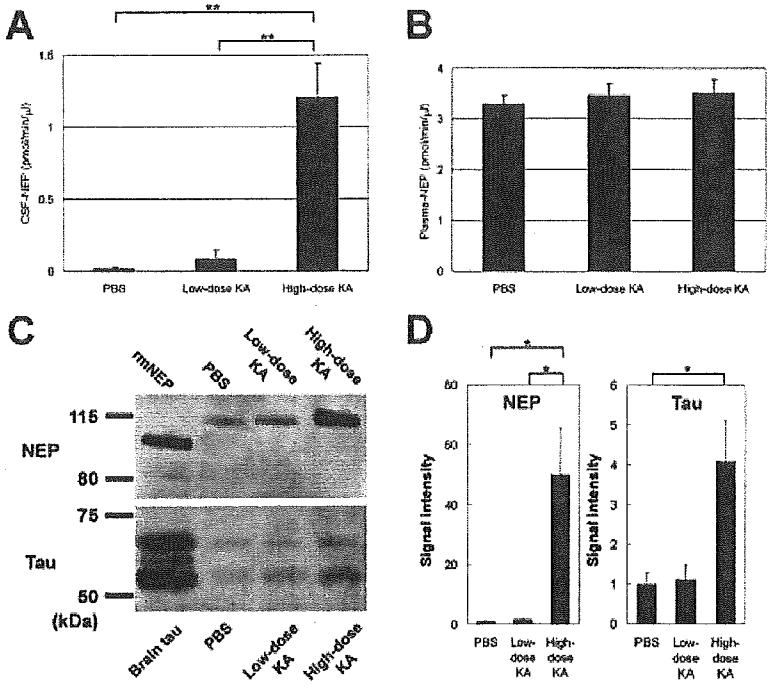

Fig 5. Increased transfer of neprilysin from the brain into cerebrospinal fluid (CSF) in a pathological condition as demonstrated by kainic acid (KA) challenge for rats. (A) Cerebrospinal fluid neprilysin activity (CSF-NEP) was increased after KA administration in a dose-dependent fashion. (B) Plasma-NEP did not significantly differ between rats injected with phosphate-buffered saline and KA. (C) Immunoblotting of neprilysin (top) also indicates a prominent increase of neprilysin in CSF from rats treated with high-dose KA. The CSF sample from a rat injected with high-dose KA was diluted fivefold, and equal volume was loaded in each lane. In addition to neprilysin, levels of tau proteins in CSF (bottom) were significantly increased in rats treated with high-dose KA. Dephosphorylated soluble fraction from rat brain tissue was applied as a control in tau immunoblotting. (D) Intensitometric data constituted from immunoblotting signals demonstrate significant increase in levels of NEP and tau in CSF from rats treated with high-dose KA. Bars *represent standard error.* $^{*}p < 0.05$; $^{**}p < 0.01$.

noreactivity (see Figs 6E, F) accompanying loss of presynaptic signals in interneurons (see Figs 6G, H) was found in the hippocampal CA1 region of the rats treated with high-dose KA compared with the control rats (merged images are shown in Figs 6I, J). These results suggest that increased CSF-NEP in KA-treated rats can be caused by pathological transfer of neprilysin from surface of injured presynaptic membrane to CSF.

Discussion

The principal outcome of this study was to demonstrate that CSF-NEP levels in patients with AD pathologies represent well both down-regulation of brain neprilysin early in the course of the aging-MCI-AD continuum and emanation of neprilysin from damaged neurons with exacerbation of the disease from early to intermediate stages. Importantly, decline of presynaptic neprilysin is putatively one of the earliest cytopathological events in AD pathogenesis[23,24] and is likely to intensify the local concentration of Aβ in the vicinity of synaptic structures. As favored by circumstantial evidence,[25] accumulation of Aβ may disrupt the integrity of synapses, conceivably causing further decrement of presynaptically localized neprilysin. In light of our findings, we conclude that CSF-NEP is potentially an informative biochemical marker to monitor this vicious cycle of synaptic pathogenesis, which can accelerate an imbalance between neprilysin activity and Aβ level in living patients with cognitive deficiency.

A literature of clinical studies has emerged indicating that CSF-tau assay permits prediction of AD-converted MCI and differentiation of prodromal AD from AD-unrelated MCI,[6,7] whereas persistent increase of CSF-tau at a nearly stable level regardless of disease stage[26] may hinder a chance to use CSF-tau as an antemortem index of neuropathological severity of AD. Unlike CSF-tau, CSF-Aβ42 is known to decline as the disease advances[6]; therefore, it may be useful to estimate magnitude of AD pathology in living patients. However, measurement of CSF-Aβ42 does not allow detection of abnormal Aβ metabolism in prodromal AD because of a great overlap among normal, sMCI, and pMCI subjects.[6,27] Based on the data obtained in this study, CSF-NEP assay is capable of distinguishing pMCI patients from normal subjects with a sensitivity of 76% and a specificity of 74% when a cutoff threshold is

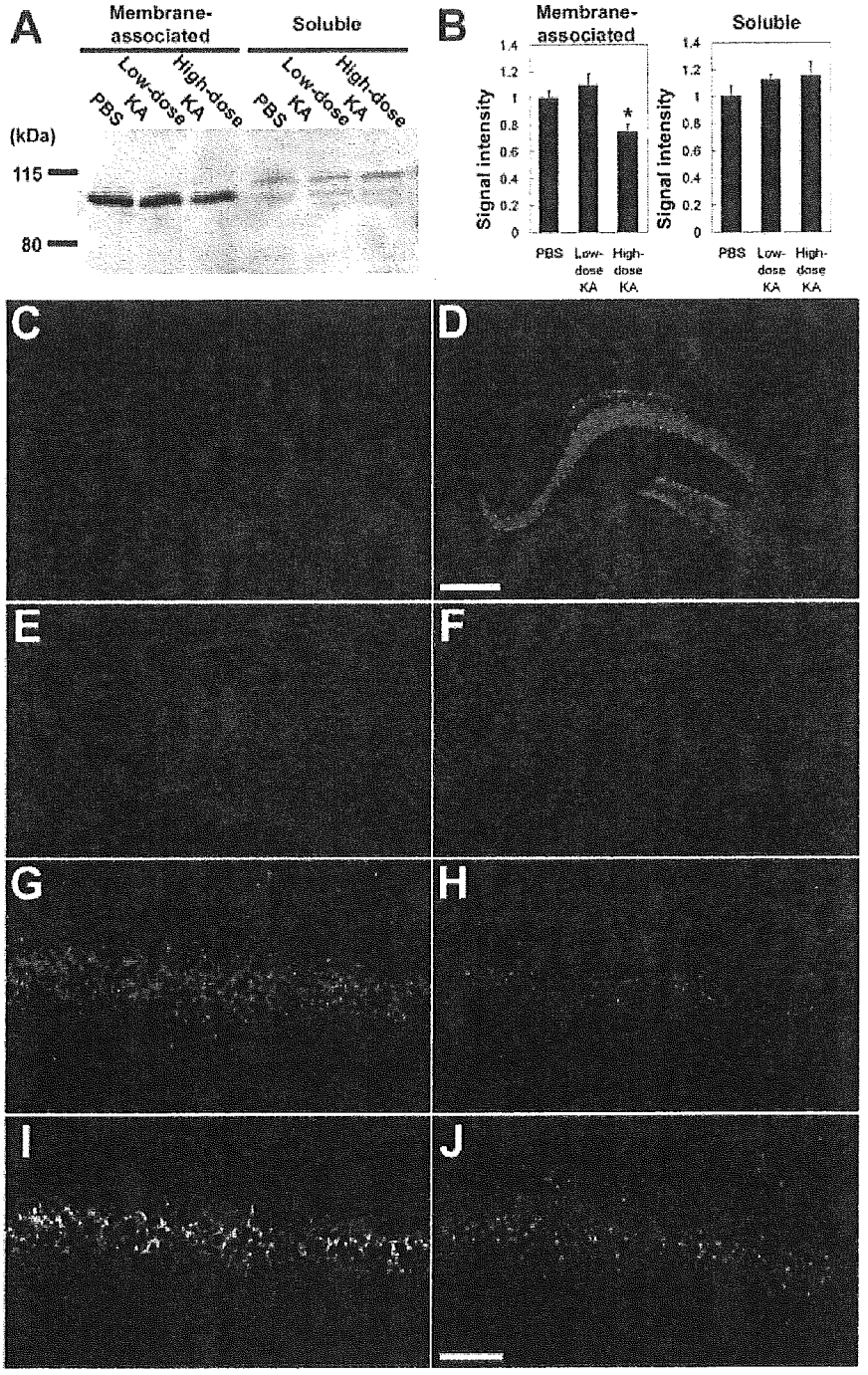

Fig 6. Reduction of neprilysin in disrupted presynaptic terminals observed in the hippocampal formations of rats treated with high-dose kainic acid (KA). (A) Representative immunoblotting indicates reduced level of membrane-associated neprilysin in high-dose KA group. Note that soluble neprilysin exhibits a larger molecular mass than membrane-associated neprilysin, presumably because of a higher magnitude of glycosylation. (B) Significant decrease of membrane-associated neprilysin in rats treated with high-dose KA was demonstrated by intensitometry of neprilysin immunoblotting signals. Bars *represent standard error. (C–J) Immunostaining of hippocampal sections from rats treated with phosphate-buffered saline (left) and high-dose KA (right). Scale bars = 250μm (C, D); 100μm (E–J).* $^{*}p < 0.05$.

assigned at 0.012 pmol/min/μl. These values may not appear particularly impressive as compared with CSF-tau, but they clearly support feasibility of using CSF-NEP as a valuable clinical adjunct to prediction of conversion from MCI to AD in view of Aβ pathogenesis. Moreover, alteration of CSF-NEP as a function of dis-

ease severity enables evaluation of neuropathological progression as patients are longitudinally examined.

It should be noted that a reduction of CSF-NEP in pMCI is indicative of a decreased level of neuronal neprilysin and a consequent diminishment of physiological transfer of neprilysin from the brain to CSF. An increased level of CSF-NEP in neprilysin-deficient mice after intrahippocampal administration of rAAV-NEP has provided unequivocal evidence for such a transfer in nonpathological conditions. The molecular mechanisms by which neprilysin is released from healthy neurons to extracellular matrix remain to be elucidated. Our immunoblotting data indicate release of neprilysin from neurons without enzymatic shedding, unlike other membrane-bound metalloproteases.[28,29] Further biochemical assessments including mass spectrometric analysis of immunocaptured samples are required to identify membrane-unbound species of neprilysin that are transferable to CSF.

As mentioned earlier, the significant association of CSF-NEP with both MMSE score and CSF-tau suggests aberrant release of neprilysin from degenerating neurons. Because there was a lack of a significant correlation between CSF-tau and MMSE score in accordance with previous findings,[26] we postulate that diffusion of neprilysin from the central nervous system to CSF in neurodegeneration has primarily two distinct origins: neurons in the middle of active neuritic and synaptic disruptions, and neurons at the end stage of the degenerative process. Based on a marked and transient increase in CSF-tau levels after acute brain injuries,[30,31] CSF-tau levels supposedly reflect the number of neurons undergoing active degenerative processes. Diffusion of neprilysin from neurons to extracellular medium can first unfold on this acute and active neuropathology, as this experiment demonstrates using KA-treated rats. Neurons at the terminal stage of degenerative changes are unlikely to release a substantial quantity of tau, because tau in such neurons is depleted in the axonal compartment or is stuck to fibrillary aggregates in the somatodendritic compartment, or both.[32] However, advanced stages of cellular injury are presumed to still allow neurons to remain productive of neprilysin, and disruption or instability of membrane structures may promote emanation of neprilysin from these cells. The number of these terminally damaged neurons increases as the disease progresses, leading to an increase of CSF-NEP in tight association with disease severity.

Our data also suggest potential benefits of neprilysin up-regulation in treating patients with pMCI and mild AD and usefulness of CSF-NEP for biochemically evaluating efficacy of the treatment in these patients. In fact, suppression of Aβ levels and amyloid plaque formation in amyloid precursor protein transgenic mice by genetically up-regulating neprilysin has been demonstrated by several independent groups.[14,33,34] Possibility of pharmacological modulation of regulatory mechanisms for neprilysin activity has also been raised by various lines of supportive evidence.[23,35] CSF-NEP could have a predictive value for identifying who would be a responder to neprilysin activation among patients with pMCI and early-stage AD.

In conclusion, this study has provided strong clinical and experimental indication that compromised neprilysin activity, Aβ-triggered neuronal injury, and a conjunction of these two changes in the brain can be monitored by CSF-NEP assay from predementia phase of AD. Quantification of CSF-NEP may also play a role in the diagnostic work-up of MCI to identify patients in transition from MCI to AD and patients afflicted by a depletion of brain neprilysin. This will be of particular importance when drugs with potential up-regulatory effects on neprilysin activity reach the clinical trial stage.

This work was supported by a grant from RIKEN BSI (M.H., Y.J., N.I.; T.S.).

We thank Dr C. Gerard at Harvard Medical School for providing neprilysin-deficient mice and M. Sekiguchi for technical assistance. We appreciate the patients and their families who made our research possible through their generous efforts to foster research.

References

1. Saido TC. Aβ metabolism: from Alzheimer research to brain aging control. In: Saido TC, ed. Aβ metabolism and Alzheimer's disease. Georgetown, TX: Landes Bioscience, 2003:1–16.
2. Hardy J, Selkoe DJ. The amyloid hypothesis of Alzheimer's disease: progress and problems on the road to therapeutics. Science 2002;297:353–356.
3. Motter R, Vigo-Pelfrey C, Kholodenko D, et al. Reduction of beta-amyloid peptide (42) in the cerebrospinal fluid of patients with Alzheimer's disease. Ann Neurol 1995;38:643–648.
4. Arai H, Terajima M, Miura M, et al. Tau in cerebrospinal fluid: a potential diagnostic marker in Alzheimer's disease. Ann Neurol 1995;38:649–652.
5. Growdon JH. Biomarkers of Alzheimer disease. Arch Neurol 1999;56:281–283.
6. Maruyama M, Arai H, Sugita M, et al. Cerebrospinal fluid amyloid beta(1-42) levels in the mild cognitive impairment stage of Alzheimer's disease. Exp Neurol 2001;172:433–436.
7. Okamura N, Arai H, Maruyama M, et al. Combined analysis of CSF tau levels and [^{123}I]iodoamphetamine SPECT in mild cognitive impairment: implications for a novel predictor of Alzheimer's disease. Am J Psychiatry 2002;159:474–476.
8. Doody RS. Current treatments for Alzheimer's disease: cholinesterase inhibitors. J Clin Psychiatry 2003;64(suppl 9):11–17.
9. Dodel RC, Hampel H, Du Y. Immunotherapy for Alzheimer's disease. Lancet Neurol 2003;2:215–220.
10. Scarpini E, Scheltens P, Feldman H. Treatment of Alzheimer's disease: current status and new perspectives. Lancet Neurol 2003;2:539–547.
11. Iwata N, Tsubuki S, Takaki Y, et al. Identification of the major $A\beta_{1-42}$-degrading catabolic pathway in brain parenchyma: suppression leads to biochemical and pathological deposition. Nat Med 2000;6:143–150.
12. Iwata N, Tsubuki S, Takaki Y, et al. Metabolic regulation of brain Aβ by neprilysin. Science 2001;292:1550–1552.

13. Fukami S, Watanabe K, Iwata N, et al. Aβ-degrading endopeptidase, neprilysin, in mouse brain: synaptic and axonal localization inversely correlating with Aβ pathology. Neurosci Res 2002;43:39–56.
14. Iwata N, Mizukami H, Shirotani K, et al. Presynaptic localization of neprilysin contributes to efficient clearance of amyloid-beta peptide in mouse brain. J Neurosci 2004;24:991–998.
15. Yasojima K, Akiyama H, McGeer EG, McGeer PL. Reduced neprilysin in high plaque areas of Alzheimer brain: a possible relationship to deficient degradation of beta-amyloid peptide. Neurosci Lett 2001;297:97–100.
16. Maruyama M, Matsui T, Tanji H, et al. Cerebrospinal fluid tau protein and periventricular white matter lesions in patients with mild cognitive impairment: implications for 2 major pathways. Arch Neurol 2004;61:716–720.
17. Petersen RC, Doody R, Kurz A, et al. Current concepts in mild cognitive impairment. Arch Neurol 2001;58:1985–1992.
18. McKhann G, Drachman D, Folstein M, et al. Clinical diagnosis of Alzheimer's disease: report of the NINCDS-ADRDA Work Group under the auspices of Department of Health and Human Services Task Force on Alzheimer's Disease. Neurology 1984;34:939–944.
19. Hama E, Shirotani K, Iwata N, Saido TC. Effects of neprilysin chimeric proteins targeted to subcellular compartments on amyloid beta peptide clearance in primary neurons. J Biol Chem 2004;279:30259–30264.
20. Edge AS. Deglycosylation of glycoproteins with trifluoromethanesulphonic acid: elucidation of molecular structure and function. Biochem J 2003;376:339–350.
21. DeMattos RB, Bales KR, Parsadanian M, et al. Plaque-associated disruption of CSF and plasma amyloid-β (Aβ) equilibrium in a mouse model of Alzheimer's disease. J Neurochem 2002;81:229–236.
22. Saido TC, Yokota M, Nagao S, et al. Spatial resolution of fodrin proteolysis in postischemic brain. J Biol Chem 1993;268: 25239–25243.
23. Saito T, Takaki Y, Iwata N, et al. Alzheimer's disease, neuropeptides, neuropeptidase, and amyloid-beta peptide metabolism. Sci Aging Knowledge Environ 2003;2003:PE1.
24. Saido TC, Nakahara H. Proteolytic degradation of Aβ by neprilysin and other peptidases. In: Saido TC, ed. Aβ metabolism and Alzheimer's disease. Georgetown, TX: Landes Bioscience, 2003:61–80.
25. Selkoe DJ. Alzheimer's disease is a synaptic failure. Science 2002;298:789–791.
26. Itoh N, Arai H, Urakami K, et al. Large-scale, multicenter study of cerebrospinal fluid tau protein phosphorylated at serine 199 for the antemortem diagnosis of Alzheimer's disease. Ann Neurol 2001;50:150–156.
27. Jensen M, Schroder J, Blomberg M, et al. Cerebrospinal fluid A β42 is increased early in sporadic Alzheimer's disease and declines with disease progression. Ann Neurol 1999;45:504–511.
28. Chubinskaya S, Mikhail R, Deutsch A, Tindal MH. ADAM-10 protein is present in human articular cartilage primarily in the membrane-bound form and is upregulated in osteoarthritis and in response to IL-1alpha in bovine nasal cartilage. J Histochem Cytochem 2001;49:1165–1176.
29. Osenkowski P, Toth M, Fridman R. Processing, shedding, and endocytosis of membrane type 1-matrix metalloproteinase (MT1-MMP). J Cell Physiol 2004;200:2–10.
30. Hesse C, Rosengren L, Vanmechelen E, et al. Cerebrospinal fluid markers for Alzheimer's disease evaluated after acute ischemic stroke. J Alzheimers Dis 2000;2:199–206.
31. Franz G, Beer R, Kampfl A, et al. Amyloid beta 1-42 and tau in cerebrospinal fluid after severe traumatic brain injury. Neurology 2003;60:1457–1461.
32. Higuchi M, Lee VM, Trojanowski JQ. Tau and axonopathy in neurodegenerative disorders. Neuromolecular Med 2002;2: 131–150.
33. Marr RA, Rockenstein E, Mukherjee A, et al. Neprilysin gene transfer reduces human amyloid pathology in transgenic mice. J Neurosci 2003;23:1992–1996.
34. Leissring MA, Farris W, Chang AY, et al. Enhanced proteolysis of beta-amyloid in APP transgenic mice prevents plaque formation, secondary pathology, and premature death. Neuron 2003; 40:1087–1093.
35. Saito T, Iwata N, Tsubuki S, et al. Somatostatin regulates brain amyloid β peptide, $A\beta_{42}$, through modulation of proteolytic degradation. Nat Med 2005;11:434–439.

ARTHRITIS & RHEUMATISM
Vol. 52, No. 1, January 2005, pp 164–170
DOI 10.1002/art.20739

Repair of Articular Cartilage Defect by Autologous Transplantation of Basic Fibroblast Growth Factor Gene–Transduced Chondrocytes With Adeno-Associated Virus Vector

Naoki Yokoo,[1] Tomoyuki Saito,[1] Masaaki Uesugi,[1] Naomi Kobayashi,[1] Ke-Qin Xin,[1] Kenji Okuda,[1] Hiroaki Mizukami,[2] Keiya Ozawa,[2] and Tomihisa Koshino[1]

Objective. **To examine the effects of basic fibroblast growth factor (bFGF) gene–transduced chondrocytes on the repair of articular cartilage defects.**

Methods. **LacZ gene or bFGF gene was transduced into primary isolated rabbit chondrocytes with the use of a recombinant adeno-associated virus (AAV) vector. These gene-transduced chondrocytes were embedded in collagen gel and transplanted into a full-thickness defect in the articular cartilage of the patellar groove of a rabbit. The efficiency of gene transduction was assessed according to the percentage of LacZ-positive cells among the total number of living cells. The concentration of bFGF in the culture supernatant was measured by enzyme-linked immunosorbent assay to confirm the production by bFGF gene–transduced chondrocytes. At 4, 8, and 12 weeks after transplantation, cartilage repair was evaluated histologically and graded semiquantitatively using a histologic scoring system ranging from 0 (complete regeneration) to 14 (no regeneration) points.**

Results. **LacZ gene expression by chondrocytes was maintained until 8 weeks in >85% of the in vitro population. LacZ-positive cells were found at the transplant sites for at least 4 weeks after surgery. The mean concentration of bFGF was significantly increased in bFGF gene–transduced cells compared with control cells ($P < 0.01$). Semiquantitative histologic scoring indicated that the total score was significantly lower in the bFGF-transduced group than in the control group throughout the observation period.**

Conclusion. **These results demonstrated that gene transfer to chondrocytes by an ex vivo method was established with the AAV vector, and transplantation of bFGF gene–transduced chondrocytes had a clear beneficial effect on the repair of rabbit articular cartilage defects.**

Damage of articular cartilage leads to joint dysfunction associated with pain or limited range of motion and usually progresses to degeneration of the articular surface, resulting in osteoarthritis. It is well recognized that articular cartilage is a highly differentiated tissue with a limited capacity for self-repair. Current therapy for osteoarthritis consists of short-acting antiinflammatory drugs, intraarticular injection of steroids or other agents, such as hyaluronic acid, and surgical intervention. However, these treatments may not relieve joint pain completely. Therefore, cartilage repair seems to be essential for the prevention of a catastrophic outcome in a joint. Several studies describing the successful repair of osteochondral defects by the transplantation of cultured chondrocytes have been reported (1). However, a major problem with cartilage repair by autologous chondrocyte transplantation is that a large quantity of chondrocytes from normal articular cartilage is required, whereas donor sites have a limited capacity to provide chondrocytes.

Supported by a grant-in-aid for Scientific Research and by the Yokohama Foundation for the Advancement of Medical Science.

[1]Naoki Yokoo, MD, Tomoyuki Saito, MD, PhD, Masaaki Uesugi, MD, PhD, Naomi Kobayashi, MD, Ke-Qin Xin, MD, PhD, Kenji Okuda, MD, PhD, Tomihisa Koshino, MD, PhD: Yokohama City University School of Medicine, Yokohama, Japan; [2]Hiroaki Mizukami, MD, PhD, Keiya Ozawa, MD, PhD: Jichi Medical School, Tochigi, Japan.

Address correspondence and reprint requests to Naoki Yokoo, MD, Department of Orthopaedic Surgery, Yokohama City University School of Medicine, 3-9 Fukuura, Kanazawa-ku, Yokohama 236-0004, Japan. E-mail: Napoleon@nyc.odn.ne.jp.

Submitted for publication February 4, 2004; accepted in revised form September 27, 2004.

Many studies have demonstrated that basic fibroblast growth factor (bFGF) is one of the most potent of the various growth factors for cartilage repair (2–6). In order to establish an efficient approach for the treatment of cartilage defects, it may be advantageous to maintain a certain level of growth factor locally for a long time.

A new therapeutic approach to cartilage repair, gene therapy, has been described, in which genes are transduced into chondrocytes with the use of naked DNA or viral vectors (7–10). However, problems with this method are related to the ability to obtain high-efficiency transduction, to maintain long-term expression of the therapeutic gene, and safety. Recently, the adeno-associated virus (AAV) has been recognized as a tool for transducing a gene into target cells (11–14). Gene therapy with AAV has several advantages, including the lack of virulence of the wild-type virus, the safety, since there is no replication activity alone, the ability to transduce to nondividing cells, the integration into the host genome, and the long-term expression of the transduced gene.

In this study, we attempted to use this new delivery vector to repair cartilage defects, in an ex vivo method. The purpose of this study was to evaluate the utility of the AAV vector for ex vivo gene delivery to chondrocytes and to investigate the repair of an articular cartilage defect by transplantation of bFGF gene–transduced chondrocytes.

MATERIALS AND METHODS

AAV vector production. Two AAV constructs were prepared for this study: AAV-LacZ contained the bacterial β-galactosidase (LacZ) gene and AAV-bFGF contained the bFGF gene, which harbors a nuclear localization signal under the regulation of the cytomegalovirus immediate early promoter. The AAV subtype 2 vector plasmid used in this study, pLacZ, was derived from the vector plasmid pW1, which contains the LacZ gene, as previously described (15). Recombinant bFGF gene (GenBank accession no. X07285) was obtained from Takeda Chemical Industries (Osaka, Japan). A fragment containing bFGF complementary DNA was amplified by polymerase chain reaction using the following primer pairs with the *Eco* RI or the *Xho* I site: 5′-ATGAATTCATGGCTGCCGGCAGCATCACTTCGCTT-3′ and 5′-ATCTCGAGAGAGTCAGCTCTTAGCAGAC-3′. The fragment was subcloned between the *Eco* RI and *Xho* I sites of the pLacZ AAV vector plasmid to replace the LacZ gene (pbFGF). An AAV helper plasmid containing subtype 2 AAV *rep* and *cap* genes, which are required for replication and capsid formation of AAV vectors, pIM45 was used. A plasmid containing the E2A, E4, and VA genes of the adenovirus genome, pladeno-1, was used in place of helper adenovirus for AAV vector production.

Subconfluent human fetal kidney cells (293 cells) were cotransfected by the calcium phosphate coprecipitation method with pbFGF, pIM45, and pladeno-1 to produce the AAV-inducing bFGF gene (AAV-bFGF). After 48 hours, the cells were harvested and lysed in Tris HCl buffer (10 m*M* Tris HCl, 150 m*M* NaCl, pH 8.0) through 3 cycles of freezing and thawing. One round of sucrose precipitation and 2 rounds of CsCl density-gradient ultracentrifugation were performed to isolate AAV-bFGF from the lysates. The vector titer was determined by quantitative DNA dot-blot hybridization of the DNase I–resistant fraction.

Isolation of chondrocytes. Thirty-nine 10-week-old Japanese white rabbits (Oriental Yeast Company, Tokyo, Japan), weighing an average of 1.8 kg, were used in this study. They were divided into 3 groups: 9 for the LacZ-transduced group, 12 for the bFGF-transduced group, and 18 for the control group. Under intravenous anesthesia with pentobarbital sodium (Somnopentyl; Schering-Plough, Union, NJ), articular cartilage tissues (4 × 4–mm slices) were harvested from the patellar groove of the right knee, washed 3 times in phosphate buffered saline (PBS), and cut into small pieces. The pieces were treated with 0.05% trypsin and 0.001*M* EDTA (Gibco BRL, Gaithersburg, MD) for 30 minutes at 37°C and digested sequentially with 0.25% collagenase (type II collagenase; Worthington, Lakewood, NJ) for 3 hours at 37°C. The isolated chondrocytes were washed 3 times with PBS.

The mean number of cells collected from each rabbit was 2.4×10^5 (SD 0.5×10^5). These cells were divided into 4–6 culture wells and cultured in 24-well flat-bottomed plates (Falcon, Lincoln Park, NJ) at a concentration of 5×10^4 cells/well in 0.5 ml of Dulbecco's modified Eagle's medium (DMEM; Sigma, St. Louis, MO) supplemented with 10% fetal calf serum (FCS) and antibiotics (100 units/ml of penicillin G, 0.1 mg/ml of streptomycin; Gibco BRL) (DMEM–FCS), at 37°C in an atmosphere of 5% CO_2 in air.

Gene transduction into chondrocytes. Chondrocytes were cultured for 3 days, removed from the growth medium, and washed once with serum-free medium. To the culture wells for the transduced group was added 500 μl of serum-free DMEM containing AAV-LacZ or AAV-bFGF to enable quantification of transgene expression at the optimal number of viral particles (10^5 particles per cell) determined from the LacZ gene group experiments. To culture wells for the control group was added 500 μl of serum-free DMEM containing Tris buffer alone. After incubation for 1 hour at 37°C, 500 μl of DMEM–FCS was added to each culture well for both culture groups. One sample from each rabbit was used for autologous transplantation. The remaining samples were used for in vitro experiments.

Twenty samples from the LacZ-transduced group and 20 from the control group were used for the experiment to determine the efficacy of gene transduction in vitro. Culture medium was exchanged twice a week after gene transduction up to the time of analysis. At 3, 7, 14, 28, and 56 days after transduction, LacZ expression was assessed using the X-Gal staining technique (16), as follows. Cells were washed 3 times with PBS and fixed with 0.5% glutaraldehyde for 10 minutes, followed by 2 rinses in PBS containing 1 mmole/liter of $MgCl_2$. The cells were finally incubated with X-Gal substrate (1 mg/ml of X-Gal, 1 mmole/liter of $MgCl_2$, 5 mmoles/liter of $K_4Fe[CN]_6/K_3Fe[CN]_6$ in PBS) for 12 hours at 37°C. Efficiency of gene transduction was calculated as the average percentage

of X-Gal–positive cells per total number of living cells in 3 randomly selected fields viewed with an optical microscope.

Measurement of bFGF concentration in culture medium. Samples from 12 rabbits in the bFGF-transduced group and from 12 rabbits in the control group were used for determinations of accumulated bFGF production in the culture supernatant. The culture medium was not changed at each sampling of either group. At 3, 7, and 14 days after transduction, culture supernatants were collected from every 4 bFGF-transduced or control group culture wells, respectively, and after centrifugation, were stored at –80°C until analyzed. The bFGF concentration in the culture supernatants was measured by enzyme-linked immunosorbent assay (ELISA) using a bFGF-specific ELISA kit (Quantikine; R&D Systems, Minneapolis, MN) according to the manufacturer's instructions.

Autologous transplantation of gene-transduced chondrocytes into an articular cartilage defect. Chondrocytes from the LacZ-transduced, bFGF-transduced, and control groups were cultured for 1 week after gene transduction, collected from the culture wells by trypsinization, and then centrifuged. The supernatant was removed, and chondrocytes were embedded in a 0.2% solution of type I collagen (Cellgen; Koken, Tokyo, Japan) at a density of 1×10^6/ml. For autologous transplantation, chondrocytes were suspended in the collagen gel by incubation at 37°C for 1 hour.

Rabbits were anesthetized with pentobarbital sodium, and the left hind leg of each rabbit was sterilized for surgery. A 3-cm medial parapatellar incision was made over the knee, and the patella was dislocated laterally. A full-thickness defect in the articular cartilage (5 mm in diameter; 3 mm deep) was made in the patellar groove using a hand drill. The collagen gel containing $\sim 7.5 \times 10^4$ autologous chondrocytes was transplanted into the full-thickness defect. A periosteal flap of $\sim 5 \times 5$ mm was harvested from the anteromedial surface of the tibia and sutured to the peripheral rim of the artificial defect with 5-0 nylon thread. The cambium layer of the periosteal flap was faced toward the joint space. The rabbits were allowed to move freely immediately after surgery.

Among the 39 rabbits, LacZ-transduced chondrocytes were transplanted into 9, bFGF-transduced chondrocytes into 12, and chondrocytes without gene transduction into the remaining 18.

Evaluation of LacZ expression at the site of transplantation. Rabbits from the LacZ-transduced (n = 3) and control (n = 2) groups were killed at 1, 2, and 4 weeks after transplantation. The specimens were harvested from the patellar groove, embedded in TissueTek OCT compound (Sakura Finetek USA, Torrance, CA), and immediately frozen in nitrogen liquid. The frozen specimens were sectioned into 20-μm slices with a cryotome (Coldtome CM-502; Sakura Seiki, Tokyo, Japan) and double-stained with X-Gal and hematoxylin and eosin (H&E).

Histologic evaluation of repair cartilage. Rabbits from the bFGF-transduced (n = 4) and control (n = 4) groups were killed at 4, 8, and 12 weeks after transplantation. The distal part of the femur was resected en bloc, fixed with 10% buffered formalin, and decalcified with a 0.5*M* EDTA solution. Sagittal sections were prepared and stained with H&E, toluidine blue, or Safranin O–fast green. The histologic features of each specimen were evaluated semiquantitatively using the histologic scoring system described by Wakitani et al (17). This system consists of 5 categories (cell morphology, matrix staining, surface regularity, cartilage thickness, and integration of donor with host) scored on a 0–14-point scale, where 0 = complete regeneration and 14 = no regeneration.

Statistical analysis. Data are expressed as the mean ± SD. The statistical significance of differences was calculated with the use of StatView software (version J-5.0; Abacus Concepts, Berkeley, CA). One-way analysis of variance and the Mann-Whitney U test were used for analyzing statistical significance. *P* values less than 0.05 were considered significant.

RESULTS

In vitro experiment. *Efficiency of gene transduction of chondrocytes.* The efficiency of gene transduction was determined for chondrocytes transfected with AAV-LacZ at 7 days after transduction. The mean ± SD percentage of LacZ-positive cells among the total number of living cells was 43.7 ± 8.8%, 62.4 ± 5.1%, 97.7 ± 0.6%, and 98.2 ± 1.5% at a vector dose of 10^3, 10^4, 10^5, and 10^6 particles/cell, respectively (Figure 1). The percentage of successfully transduced chondrocytes increased in a vector dose–dependent manner. A vector dose of $>10^6$ particles/cell did not improve the transduction rate. The optimal dose of virus that was required to achieve transduction of ~100% of the chondrocytes was determined to be 10^5 particles/cell.

LacZ gene expression was highly maintained until 56 days after gene transduction. The mean ± SD percentage of LacZ-positive cells was 69.4 ± 15.1%, 97.7 ± 0.6%, 97.2 ± 1.8%, 95.8 ± 2.9%, and 85.8 ± 6.2% at 3, 7, 14, 28, and 56 days after transduction, respectively (Figure 2). The greatest population of

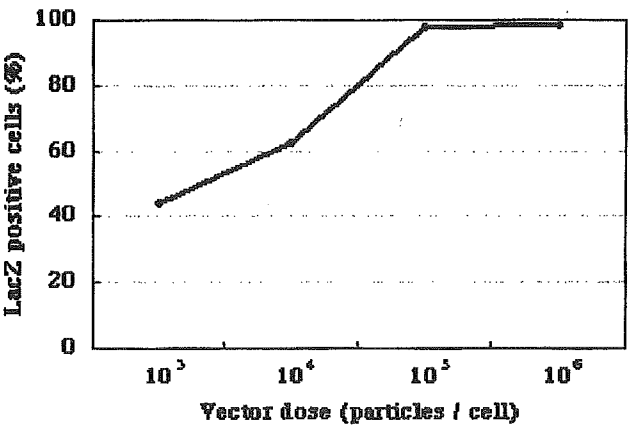

Figure 1. Vector dose–dependent LacZ expression in cultured chondrocytes. On day 7 after adeno-associated virus–LacZ transduction into chondrocytes, LacZ expression was assessed by X-Gal staining. The percentages of LacZ-positive cells among the total number of living cells were 43.7%, 62.4%, 97.7%, and 98.2% at doses of 10^3, 10^4, 10^5, and 10^6 particles/cell, respectively.

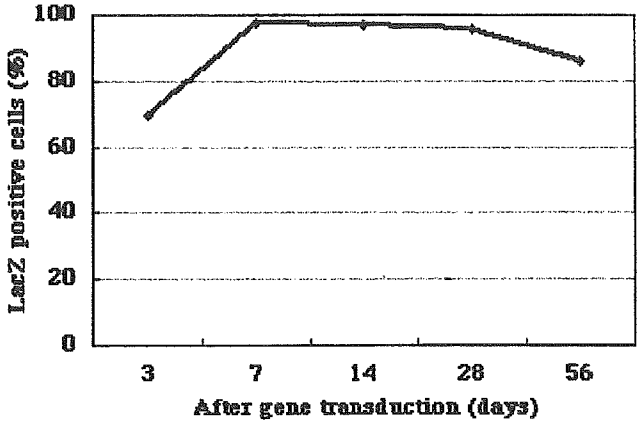

Figure 2. Time-dependent expression of LacZ in cultured chondrocytes. The percentages of LacZ-positive cells were 69.4%, 97.7%, 97.2%, 95.8%, and 85.8% at 3, 7, 14, 28, and 56 days after transduction, respectively.

LacZ-expressing cells was 97.7% at 7 days (Figure 3A), and more than 85% of the population was maintained up to 56 days. Cells without LacZ transduction in the control group failed to reveal LacZ expression at any sampling point (Figure 3B). There was no microscopic evidence of cell death or cytopathologic changes in the transduced cells as determined by optical microscopy.

Expression of bFGF gene by transduced chondrocytes. Production of bFGF was detected in both bFGF-transduced cells and control cells. The mean ± SD bFGF concentration in culture supernatants from the bFGF-transduced cells was 88.2 ± 9.8 ng/ml, 130.9 ± 28.8 ng/ml, and 240.6 ± 22.5 ng/ml at 3, 7, and 14 days after transduction, respectively (Figure 4). In control

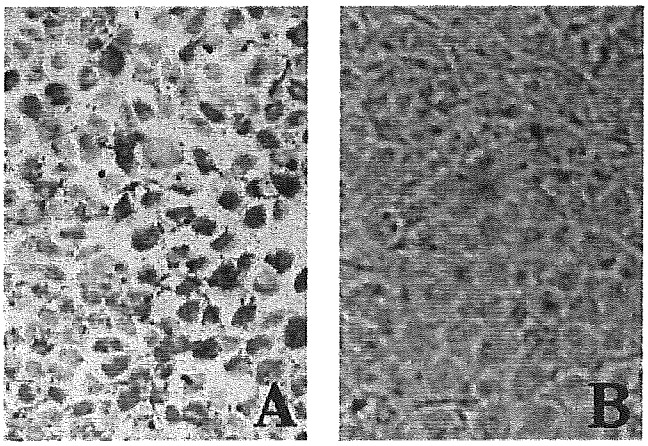

Figure 3. Photomicrographs of transduced chondrocytes stained with X-Gal. **A,** LacZ group chondrocytes were stained with X-Gal on day 7 after adeno-associated virus–LacZ transduction. LacZ-positive cells are stained blue. **B,** Control group chondrocytes showed no LacZ-positive cells. (Original magnification × 100.)

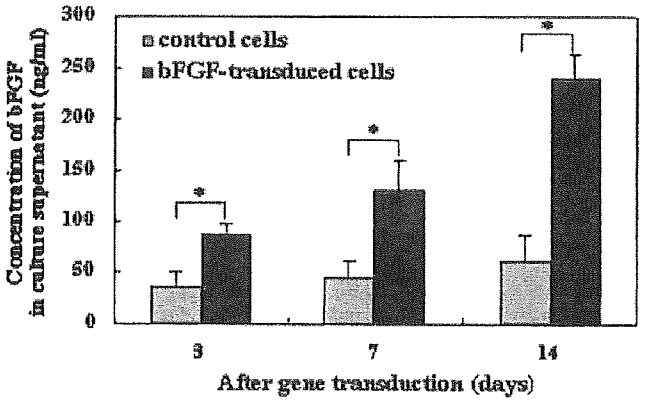

Figure 4. Concentration of basic fibroblast growth factor (bFGF) in culture supernatants of bFGF-transduced chondrocytes. Culture supernatants of control and bFGF-transduced cells were collected on days 3, 7, and 14 after transduction, and the bFGF concentration was determined by enzyme-linked immunosorbent assay. Transduction of the bFGF gene significantly elevated the secretion of bFGF (* = $P <$ 0.01).

cells, the bFGF concentration was 35.0 ± 15.8 ng/ml, 44.5 ± 16.4 ng/ml, and 62.3 ± 25.8 ng/ml at 3, 7, and 14 days after transduction, respectively. The bFGF concentration was significantly greater in bFGF-transduced cells than in the control cells on all sampling days ($P <$ 0.01).

The mean number of chondrocytes in the bFGF-transduced group was 14.1 × 10^4 (SD 1.1 × 10^4) and 34.8 × 10^4 (SD 6.2 × 10^4) at 7 and 14 days after transduction, respectively. In the control group, the numbers were 6.4 × 10^4 (SD 1.5 × 10^4) and 17.0 × 10^4 (SD 3.2 × 10^4) at 7 and 14 days after transduction, respectively. The mean number of chondrocytes in the bFGF-transduced group was significantly higher than that in the control group during the period of culture ($P <$ 0.01).

In vivo experiment. *LacZ expression at the transplant site.* Throughout the observation period, X-Gal staining of LacZ-transduced cells showed cells with blue nuclei distributed across the entire regenerated cartilage under the layer covered by the transplanted periosteal flap. The controls, which received transplants without LacZ-transduced chondrocytes, did not show LacZ-positive cells at any week of sampling. No adverse effects related to the virus were observed in this ex vivo gene transfer experiment.

Macroscopic findings at the site of transplantation of the bFGF-transduced chondrocytes. Macroscopic observation of the transplant site showed regeneration of the articular cartilage defect in both the bFGF-transduced and control groups. At 12 weeks, the margin between the regenerated tissue and the

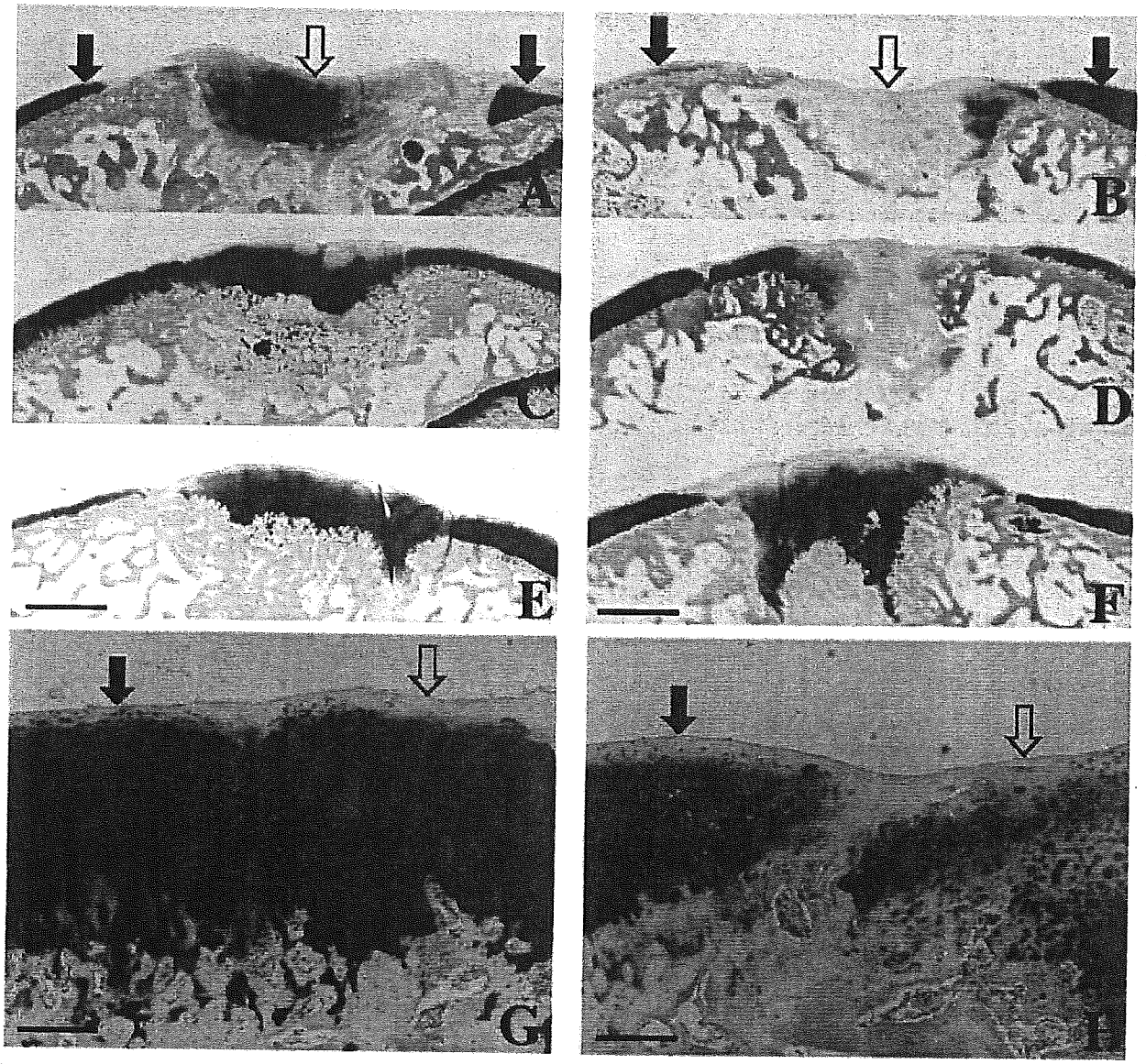

Figure 5. Photomicrographs of sagittal sections of articular cartilage defects in rabbits after transplantation with basic fibroblast growth factor (bFGF)–transduced chondrocytes (**A, C, E,** and **G**) and control chondrocytes (**B, D, F,** and **H**). Photomicrographs of the junction area are also shown (**G** and **F**). In the bFGF-transduced group, at 4 weeks (**A**), the deep layer is composed of round chondrocytes, but the matrix is weakly stained. At 8 weeks (**C**), the matrix is more distinctly stained, but the superficial region is weakly stained. At 12 weeks (**E** and **G**), the matrix is intensely metachromatically stained, and there is reconstitution of the osteochondral junction in most specimens. In the control group, at 4 weeks (**B**) and 8 weeks (**D**), the matrix is faintly stained. At 12 weeks (**F** and **H**), the deep layer of the matrix stained well, but staining is reduced in the superficial layers. **Solid arrows** indicate regenerated cartilage; **open arrows** indicate surrounding normal cartilage. Sections were stained with Safranin O–fast green. Bars in **A** and **F** = 1 mm; bars in **G** and **H** = 100 μm.

original cartilage was not distinguishable in both groups. The surface of the regenerated cartilage closely resembled normal cartilage in the bFGF-transduced group, but that in the control group could still be distinguished from surrounding normal cartilage. No sign of osteoarthrosis, such as erosion of cartilage or osteophyte formation, was seen in any of the knees during the observation period.

Histologic findings of regenerated cartilage following transplantation of bFGF-transduced chondrocytes. At 4 weeks after transplantation, in the tissues obtained from the bFGF-transduced group, the deep part of the

Table 1. Histologic scores of regenerated cartilage at 4, 8, and 12 weeks*

Weeks after transplantation	Control group	bFGF-transduced group
4	8.8 ± 1.0	6.5 ± 0.6†
8	7.0 ± 1.4	4.3 ± 1.0†
12	5.5 ± 1.7	2.8 ± 1.0†

* The histologic features were scored on a 0–14-point scale as described by Wakitani et al (17), where 0 represents complete regeneration and 14 represents no regeneration. Values are the mean ± SD. bFGF = basic fibroblast growth factor.
† $P < 0.01$ versus controls.

regenerated tissue was composed of round chondrocytes, with an extracellular matrix that stained weakly with Safranin O (Figure 5A). There was no integration of the edges of the regenerated tissue with the adjacent normal cartilage or reconstitution of the osteochondral junction in any specimen. In the control group, the extracellular matrix was faintly stained with Safranin O (Figure 5B).

At 8 weeks, the bFGF-transduced group showed an extracellular matrix that was more distinctly stained with Safranin O in the deep part, while the superficial part was weakly stained (Figure 5C). Although both edges were integrated with the adjacent normal cartilage, reconstitution of the osteochondral junction was not seen in any specimen. The tissues from the control group at 8 weeks were essentially the same as those at 4 weeks (Figure 5D).

In the bFGF-transduced group at 12 weeks, the intensity and thickness of the extracellular matrix that was metachromatically stained with Safranin O were increased as compared with the findings at 4 and 8 weeks, and the microstructure of the regenerated tissue resembled the surrounding normal cartilage (Figures 5E and G). There was reconstitution of the osteochondral junction in most of the specimens. In the control group, the deep layer of the regenerated cartilage matrix stained well with Safranin O, but staining was reduced in the superficial layers (Figures 5F and H). There was no reconstitution of the osteochondral junction in any of the control specimens.

The Wakitani score was 6.5 ± 0.6, 4.3 ± 1.0, and 2.8 ± 1.0 points (mean ± SD) at 4, 8, and 12 weeks after transplantation, respectively, in the bFGF-transduced group. In the control group, the score was 8.8 ± 1.0, 7.0 ± 1.4, and 5.5 ± 1.7 points at 4, 8, and 12 weeks after transplantation, respectively (Table 1). The scores in both groups gradually decreased throughout the experimental period. However, the score in the bFGF-transduced group became significantly lower than that in the control group with the passage of time postoperatively ($P < 0.01$).

DISCUSSION

Autologous chondrocyte transplantation has been successfully applied in recent years to the treatment of focal cartilage defects in a series of patients (18). Autologous chondrocytes for grafting are harvested from non–weight-bearing areas, cultured in vitro, reinjected into the cartilage defect, and the area is covered with a periosteal flap that is sutured in place. However, this method may be limited to small local cartilage defects, since the number of cells collected from donor sites to be used for cultivation is still limited.

Augmentation of the procedure with bFGF for help in repairing the cartilage has been reported to be efficacious (4–6,19). Weisser et al (4) reported that among several different growth factors used to treat transplanted chondrocytes, positive effects on cartilage repair were observed only with the bFGF-treated chondrocyte implants (4). Previous studies showed that exogenous bFGF induces the proliferation of chondrocytes, the maturation of cartilage, and the differentiation of mesenchymal cells, and it stimulates the synthesis of cartilaginous matrix (5,6). Otsuka et al (19) reported that continuous administration of bFGF using an osmotic pump had a clearly beneficial effect on repair of cartilage defects. However, bFGF alone did not lead to complete structural restitution of hyaline cartilage to repair the full-thickness defects of articular cartilage. Prolonged local expression of bFGF by transduction of the genetic code of bFGF into chondrocytes would be an efficient treatment for articular cartilage defects.

For the repair of cartilage defects with gene therapy, it may be necessary to obtain high-efficiency transduction and continuous local expression of the therapeutic gene. Several studies have demonstrated that the AAV vector has the ability to highly efficiently transduce a gene into cells, to integrate into the host genome, and to express the transduced gene for a long time (20–22). There are studies of the utility of the AAV vector for joint disease that demonstrated high-efficiency gene delivery to the synovium in vivo (23) or gene transduction to cultured chondrocytes in vitro (24). Delivering genes directly to the surface of the abnormal articular cartilage in order to accelerate cartilage repair could result in a long-term treatment. The advantage of ex vivo gene delivery would be direct delivery of the therapeutic gene to the abnormal articular cartilage and the ability to limit the area of gene expression to the cartilage defect alone. In our previous study, ex vivo

gene transfer to periosteum-derived cells using an AAV vector induced LacZ expression for 4 weeks in vivo (25).

In this study, high-efficiency LacZ gene transduction into chondrocytes was obtained long-term in vitro, and LacZ gene expression in vivo was sustained without any adverse effects. These findings suggest that gene transfer to an articular cartilage defect by use of the ex vivo method was established with the AAV vector. Cartilage repair was slightly inferior to that described in previous reports, even though we used 10-week-old rabbits for the experiment. One of the reasons was thought to be differentiation to fibrous chondrocytes during the 1-week culture before transplantation. The cell number and the bFGF secretion were significantly increased in bFGF-transduced chondrocytes compared with the control chondrocytes in vitro. Furthermore, the histologic appearance of the transplant site in the bFGF-transduced group was fully repaired compared with that in the control group. The repair at a comparatively early stage was apparently different between bFGF-transduced and null chondrocytes even at 12 weeks. Continuous bFGF secretion by gene transfer seemed to be an effective way to promote cartilage repair.

These results demonstrate that repair of full-thickness defects in rabbit articular cartilage can be enhanced by transplantation of bFGF gene–transduced chondrocytes. This method seems to be one of the best techniques for achieving repair of articular cartilage defects.

ACKNOWLEDGMENT

We thank Avigen, Inc. (Alameda, CA) for supplying the plasmid for the production of the AAV vector.

REFERENCES

1. Brittberg M, Lindahl A, Nilsson A, Ohlsson C, Isaksson O, Peterson L. Treatment of deep cartilage defects in the knee with autologous chondrocyte transplantation. N Engl J Med 1994;331: 889–95.
2. Kato Y, Gospodarowicz D. Sulfated proteoglycan synthesis by confluent cultures of rabbit costal chondrocytes grown in the presence of fibroblast growth factor. J Cell Biol 1985;100:477–85.
3. Hunziker EB, Rosenberg LC. Repair of partial-thickness defects in articular cartilage: cell recruitment from the synovial membrane. J Bone Joint Surg Am 1996;78:721–33.
4. Weisser J, Rahfoth B, Timmermann A, Aigner T, Brauer R, von der Mark K. Role of growth factors in rabbit articular cartilage repair by chondrocytes in agarose. Osteoarthritis Cartilage 2001; 9:48–54.
5. Shida J, Jingushi S, Izumi T, Iwaki A, Sugioka Y. Basic fibroblast growth factor stimulates articular cartilage enlargement in young rats in vivo. J Orthop Res 1996;14:265–72.
6. Cuevas P, Burgos J, Baird A. Basic fibroblast growth factor (FGF) promotes cartilage repair in vivo. Biochem Biophys Res Commun 1988;156:611–8.
7. Arai Y, Kubo T, Kobayashi K, Takeshita K, Takahashi K, Ikeda T, et al. Adenovirus vector-mediated gene transduction to chondrocytes: in vitro evaluation of therapeutic efficiency of transforming growth factor-β1 and heat shock protein 70 gene transduction. J Rheumatol 1997;24:1787–95.
8. Baragi VM, Renkiewicz RR, Qiu L, Brammer D, Riley JM, Sigler RE, et al. Transplantation of adenovirally transduced allogeneic chondrocytes into articular cartilage defects in vivo. Osteoarthritis Cartilage 1997;5:275–82.
9. Doherty PJ, Zhang H, Tremblay L, Manolopoulos V, Marshall KW. Resurfacing of articular cartilage explants with genetically-modified human chondrocytes in vitro. Osteoarthritis Cartilage 1998;6:153–9.
10. Kang BR, Marui T, Ghivizzani SC, Nita IM, Georgescu HI, Suh JK, et al. Ex vivo gene transfer to chondrocytes in full-thickness articular cartilage defects: a feasibility study. Osteoarthritis Cartilage 1997;5:139–43.
11. Schwarz EM. The adeno-associated virus vector for orthopaedic gene therapy [review]. Clin Orthop 2000;379 Suppl:S31–9.
12. Kaplitt MG, Leone P, Samulski RJ, Xiao X, Pfaff DW, O'Malley KL, et al. Long-term gene expression and phenotypic correction using adeno-associated virus vectors in the mammalian brain. Nat Genet 1994;8:148–54.
13. Xiao X, Li J, McCown TJ, Samulski RJ. Gene transfer by adeno-associated virus vectors into the central nervous system. Exp Neurol 1997;144:113–24.
14. Berns KI, Giraud C. Adenovirus and adeno-associated virus as vectors for gene therapy. Ann N Y Acad Sci 1995;772:95–104.
15. Xin KQ, Urabe M, Yang J, Nomiyama K, Mizukami H, Hamajima K, et al. A novel recombinant adeno-associated virus vaccine induces a long-term humoral immune response to HIV. Hum Gene Ther 2001;12:1047–61.
16. Price J, Turner D, Cepko C. Lineage analysis in the vertebrate nervous system by retrovirus-mediated gene transfer. Proc Natl Acad Sci U S A 1987;84:156–60.
17. Wakitani S, Goto T, Pineda SJ, Young RG, Mansour JM, Caplan AI, et al. Mesenchymal cell-based repair of large, full-thickness defects of articular cartilage. J Bone Joint Surg Am 1994;76: 579–92.
18. Richardson JB, Caterson B, Evans EH, Ashton BA, Roberts S. Repair of human articular cartilage after implantation of autologous chondrocytes. J Bone Joint Surg Br 1999;81:1064–8.
19. Otsuka Y, Mizuta H, Takagi K, Iyama K, Yoshitake Y, Nishikawa K. Requirement of fibroblast growth factor signaling for regeneration of epiphyseal morphology in rabbit full-thickness defects of articular cartilage. Dev Growth Differ 1997;39:143–56.
20. Kessler PD, Podsakoff GM, Chen X, McQuiston SA, Colosi PC, Matelis LA, et al. Gene delivery to skeletal muscle results in sustained expression and systemic delivery of a therapeutic protein. Proc Natl Acad Sci U S A 1996;93:14082–7.
21. Fisher KJ, Jooss K, Alston J, Yang Y, Haecker SE, High K, et al. Recombinant adeno-associated virus for muscle directed gene therapy. Nat Med 1997;3:306–12.
22. Herzog RW, Hastrom JN, Kung SH, Tai SJ, Wilson JM, Fisher KJ, et al. Stable gene transfer and expression of human blood coagulation factor IX after intramuscular injection of recombinant adeno-associated virus. Proc Natl Acad Sci U S A 1997;94:5804–9.
23. Goater J, Muller R, Kollias G, Firestein GS, Sanz I, O'Keefe RJ, et al. Empirical advantages of adeno associated viral vectors for in vivo gene therapy for arthritis. J Rheumatol 2000;27:983–9.
24. Arai Y, Kubo T, Fushiki S, Mazda O, Nakai H, Iwaki Y, et al. Gene delivery to human chondrocytes by an adeno associated virus vector. J Rheumatol 2000;27:979–82.
25. Kobayashi N, Koshino T, Uesugi M, Yokoo N, Xin KQ, Okuda K, et al. Gene marking in adeno-associated virus vector infected periosteum-derived cells for cartilage repair. J Rheumatol 2002; 29:2176–80.